Carbohydrate Polymers 89 (2012) 830–835

Contents lists available at SciVerse ScienceDirect

Carbohydrate Polymers

journal homepage: www.elsevier.com/locate/carbpol

Synthesis of worm like silver nanoparticles in methyl cellulose polymeric matrix and its catalytic activity

Dipak Kumar Bhui, Ajay Misra*

Department of Chemistry and Chemical Technology, Vidyasagar University, Midnapore 721 102, W.B., India

ARTICLE INFO

Article history:
Received 27 January 2012
Received in revised form 6 April 2012
Accepted 7 April 2012
Available online 16 April 2012

Keywords:
Silver nanoparticles
Methyl cellulose (MC)
Surface plasmon resonance (SPR)
Catalytic activity

ABSTRACT

A facile one step method for the synthesis of wormlike silver nanoparticles has been carried out in methyl cellulose matrix. Synthesis is based on the reduction of $AgNO_3$ by sodium borohydride ($NaBH_4$) in aqueous methyl cellulose (MC). Synthesized nanoparticles are mostly mono disperse in size and their aggregation is controlled by varying the concentration of $AgNO_3$. Silver nanoparticles are analyzed using transmission electron microscope (TEM), UV–vis spectroscopy and X-ray diffraction (XRD) technique. It has been found that the concentration of $AgNO_3$ has a significant effect on the morphology of Ag nanostructures. Worm like nanostructures showed excellent catalytic activity in the borohydride reduction of p-nitrophenol compared to spherical shaped nanoparticles.

1. Introduction

During the last two decades, research on inorganic nanoparticles has been developing rapidly due to their exceptional physical and chemical properties that are quite different from the bulk one (Ozin, 1992). Among the noble metal nanoparticles silver is perhaps the most widely recognized for its unique optical properties, as manifested by its central role in photography (Kreibig & Vollmer, 1995). Study of silver nanoparticles has led to significant advancement in the area such as photonics (Gould et al., 2000; Lin & Wang, 1996; Wang & Toshima, 1997), micro-electronics (Deheer, 1993; Schimd, 1992), lithography (Shipway et al., 2000; Xia, Rogers, Paul, & Whitesides, 1999), drug delivery (Mann & Ozin, 1996), optics (Jensen, Malinsky, Haynes, & Van Duyne, 2000; Ramakrishna & Ghosh, 2003), catalysis (Bawendi, Steigerwald, & Brus, 1990; Kayanuma, 1988; Narayanan & El-Sayed, 2004; Rashid, Bhattacharjee, Kotal, & Mandal, 2006), etc.

In nanoscale regime, chemical and physical properties of inorganic crystals are highly dependent on factors such as sizes and shapes. Precise controls of such factors allow not only to observe unique properties of nanocrystals but also to tune their chemical and physical properties as desired. A large variety of synthetic approaches have been explored for the preparation of silver nanoparticles with different morphologies, such as hydrothermal (Sun, Mayers, & Xia, 2003; Yu & Yam, 2004), microemulsion (Andersson, Pederson, & Palmgrist, 2005), electrochemical deposition (Liu & Lin, 2004; Sandmann, Dietz, & Plieth, 2000), photochemical (Keki, Torok, Deak, Daroczi, & Zsuga, 2000; Mallick, Witcomb, & Scurrell, 2005), γ-ray irradiation (Temgire & Joshi, 2004), etc. Among these approaches 'hard and soft' templates are commonly used in order to obtain silver nanoparticles with variable morphologies. For examples, silver nanowires can be prepared within 'hard' templates, such as porous alumina membranes, carbon nanotubes and block copolymer (Gobindaraj, Satishkumar, Nath, & Rao, 2000; Zhang, Qi, Ma, & Cheng, 2001; Zong et al., 2004). Alternatively a range of 'soft' templates, such as PVP (Sun et al., 2003), CTAB (Yu & Yam, 2004), bis(p-sulfonatophenyl) phenylphosphine dehydrate dipotassium salt solution (Jin et al., 2001), SDS (Bhui et al., 2009; Samanta et al., 2010), unsaturated isomeric dicarboxylates (Sarkar et al., 2009), HPMC (Sarkar et al., 2011) and MC (Bhui et al., 2011; Sahoo et al., 2010) have been used to prepare silver nanostructures of various morphologies. On the other hand, seed mediated growth process has been extensively used to synthesize silver nanowire (Gou, Chipara, & Zaleski, 2007; Sun, Gates, Mayers, & Xia, 2002), nanocube (Wiley, Sun, & Xia, 2005) and nanorods (Sun et al., 2003; Sarkar et al., 2011). Though the reports on morphology-controlled synthesis of silver nanoparticles are quite abundant, still there are enough scope for the morphology-controlled synthesis of silver nanoparticles in terms of its purity and monodispersity.

In this article, we report a simple one step method to synthesize silver nanostructures from aqueous solution of silver nitrate ($AgNO_3$) and methyl cellulose (MC). Methyl cellulose is used instead

---

* Corresponding author. Fax: +91 3222 275329.
E-mail addresses: ajaymsr123@gmail.com, ajaymsr@yahoo.co.in (A. Misra).

0144-8617/$ – see front matter © 2012 Elsevier Ltd. All rights reserved.
http://dx.doi.org/10.1016/j.carbpol.2012.04.017

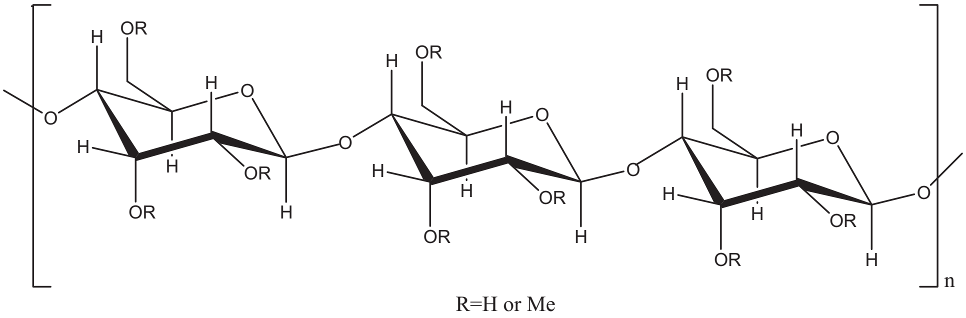

Scheme 1. Chain structure of methyl cellulose.

of cellulose, because cellulose itself is insoluble in water and also in most organic solvents. But MC is water soluble, easily prepared by controlled methylation of cellulose, nontoxic and renewable capping agent. The structure of the MC (Scheme 1) shows that there are linear chains with β-(1→4) linkage with one free-OH and two free-OCH_3 group per unit. The absence of strong reducing group insists us to use sodium borohydride for the reduction of $AgNO_3$. Due to the β-linkage, the methylated glucose unit in MC is flipped over. This enhances the intra and inter chain hydrogen bonding and is responsible for the MC chain to be rigid and packed with crystalline arrangement of thick bundles, called micro fibrils. The as-prepared Ag-nanoparticles are adsorbed on the surface of microfibrils. We carried out the synthesis with two different concentration of $AgNO_3$ at 0 °C. The synthesize particles are small and almost spherical at lower concentration and wormlike nanostructures at higher concentration of $AgNO_3$.

In recent years, several research groups have investigated the catalytic reduction of aromatic nitro compounds using a number of noble metal nanoparticles (Esumi, Isono, & Yoshimura, 2004; Hayakawa, Yoshimura, & Esumi, 2003; Jana et al., 2006; Liu, Qin, Raveendran, & Ikushima, 2006; Pradhan, Pal, & Pal, 2002; Praharaj, Nath, Ghosh, Kundu, & Pal, 2004). However, in most of the cases, metal nanoparticles were supported either by dendrimer/polymers or resin prior to catalysis reduction (Esumi et al., 2004; Hayakawa et al., 2003; Jana et al., 2006; Praharaj et al., 2004) and most of the nanoparticles are spherical. Thus, for the first time we report the use of worm like Ag nanostructures as an efficient catalyst for the reduction of p-nitrophenol to p-aminophenol by $NaBH_4$.

2. Materials and methods

2.1. Chemicals

Silver nitrate was purchased from Sigma–Aldrich Chemical corp. and was used without further purification. Methyl cellulose (MC) was purchased from Merck India Ltd. and recrystallized from methanol/water mixture before use. Sodium borohydride was purchased from S.D. Fine-Chem. Ltd. p-Nitrophenol was obtained from Merck India Ltd. All solutions were prepared in triply distilled de-ionized water.

2.2. Preparation of methyl cellulose (MC) solution

85 mg methyl cellulose (average molecular weight: 3,20,000–3,50,000; degree of polymerization: 4000 cps; viscosity: 2% (w/v) in water at 20 °C) was taken in a 100 ml round bottom flask. It was heated to 80 °C with triply distilled deionized water for 1 h. The turbid solution was kept in deep freeze for an hour and clear MC solution was obtained.

2.3. Preparation of nanoparticles

10 ml 1 mM $AgNO_3$ solution was added to the freshly prepared 10 ml MC (0.085%) solution and the mixture was stirred for 10 min under ice cold condition. Then 5 ml 0.1 (M) $NaBH_4$ was added drop wise with continuous stirring at 0 °C to the above mixture. After the complete addition of sodium borohydride the yellow colored silver hydrosol was obtained and it was brought to normal temperature. The above procedure was repeated using 10 ml 10 mM $AgNO_3$ and surprisingly the color obtained for silver hydrosol was green. This difference in color indicates the formation of different nanostructures of Ag nanoparticles.

2.4. Studies of catalytic activity

Catalytic activities of the as synthesized AgNPs were carried out by measuring $NaBH_4$ reduction of p-nitrophenol (p-NP) in presence of Ag NPs. In order to study catalytic activity, 10 ml of p-NP (0.4 μM) was mixed with a freshly prepared aqueous solution of $NaBH_4$ (0.10 ml, 0.3 M) with constant stirring in a 25 ml conical flask. Then, 0.3 ml each of the as prepared Ag nano hydrosol was added to the mixture separately and the conical flask was shaken vigorously for mixing.

The color of the solutions was changed gradually from yellow to colorless as the reaction proceeded. The progress of the reaction was monitored by recording the UV–vis spectra of the solution at a time interval of 60 s. The controlled experiment was also carried out without AgNPs and we noticed no change in the absorption spectra of p-NP.

2.5. Physical characterization

Transmission electron microscopic study for the characterization of particles was carried out by placing a drop of silver sol onto a carbon film supported on a copper grid, followed by solvent evaporation under vacuum. Samples were studied using a JEOL-JEM-2100 transmission electron microscope (TEM). Absorption spectral measurements were done using Shimatzu (model no. UV1601) UV–vis spectrophotometer. X-ray diffraction studied was carried out using X'Pert PRO PAnalytical-PW 3040/60 X-ray diffractometer with Cu Kα radiation (λ = 0.154056 nm). Samples for XRD study were prepared by deposition of colored hydrosol on silica glass slide and then kept in vacuum. Finally the slide was heated and then cooled to study the diffraction spectra.

3. Results and discussion

3.1. UV–vis spectra

Formation and the stability of silver nanoparticles in aqueous colloidal solution are confirmed by UV–vis spectral analysis. The

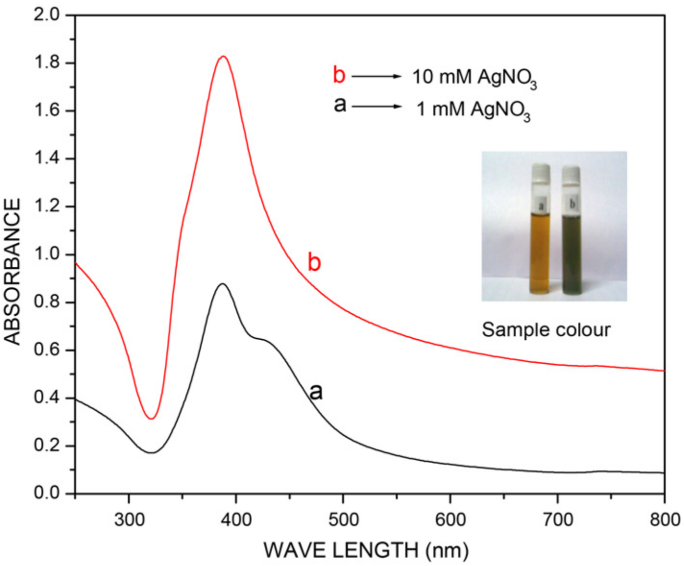

Fig. 1. UV–vis extinction spectra of the silver hydrosol synthesized from (a) 1 mM $AgNO_3$ and (b) 10 mM $AgNO_3$ in MC solution (inset shows the corresponding color of the as prepared silver nanosols).

UV–vis spectra of silver nanoparticles synthesized from different concentration of silver nitrate are shown in Fig. 1. Characteristic surface plasmon resonance (SPR) absorption band is observed at 426 nm and 388 nm, respectively, for yellowish colored silver nanoparticles synthesized from 1 mM silver nitrate. Overlapping SPR band suggests the presence of two different size distributions of AgNPs and it is further confirmed by our TEM measurements (Fig. 2). On the other hand, the SPR band of silver hydrosol synthesized using 10 mM $AgNO_3$ maximizes at 388 nm with a long tail showing absorption >800 nm. This long tail absorption along with the 388 nm band indicates the anisotropic nature of AgNP and the long tail absorption due to longitudinal SPR absorption (Gou et al., 2007).

3.2. TEM study

Effect of concentration on the shape, size and dispersity of Ag-nanoparticles is truly noticeable from the TEM images. Fig. 2a shows the TEM image of the as prepared silver nanoparticles synthesized from 1 mM $AgNO_3$. It is obvious from the bar diagram (Fig. 2b) that most of the silver nanoparticles are spherical with diameter ranging from 6 to 10 nm (50%) and 16 to 22 nm (50%) and it again supports the two maxima of SPR band. Polycrystalline nature of silver nanoparticles has been supported by the selected area electron diffraction (SAED) image as shown in the inset of Fig. 2a. Worm like nanostructures are formed when the concentration of $AgNO_3$ is 10 mM (Fig. 3a). Fig. 3b shows the corresponding SAED image and it supports the crystalline nature of the as prepared silver nanostructures. We believe that the nanostructures are absorbed and stabilized on the MC bundle which is formed by chemical derivatization (Ruan, Zhang, Zhang, & Xia, 2004).

3.3. XRD study

Fig. 4a and b shows the XRD patterns of vacuum dried silver nanoparticles obtained from 1 mM and 10 mM $AgNO_3$, respectively. Fig. 4a shows that a number of Bragg reflections with 2θ values of 38.2°, 44.0° and 64.5° sets of lattice planes are observed which can be indexed to the (1 1 1), (2 0 0) and (2 2 0) facets of the band for face centered cubic (fcc) structure of silver. Again from Fig. 4b, the observed 2θ values are 38.2°, 44.5°, 64.5° and 77.4° and these are from (1 1 1), (2 0 0), (2 2 0) and (3 1 1) lattice planes of fcc crystalline structure of AgNP. The peak intensity of the (1 1 1) plane ($2\theta = 38.2°$) is very high and this is due to the preferential adsorption of Ag atom on that plane during the growth process.

3.4. Catalytic activity studies of silver nanostructures

Catalytic activities of AgNPs for the conversion of p-nitrophenol to p-aminophenol (p-AP) in presence of $NaBH_4$ were studied by monitoring the UV–vis absorption spectra of both the species. Fig. 5a displays the evolution of the UV–vis spectra with time in the presence of spherical Ag nanoparticles. Similar results have been obtained when the worm like Ag nanostructures act as catalyst (Fig. 5b). The isosbestic points in the UV–vis spectra (Fig. 5a and b) demonstrate with high precision that p-NP is converted to p-AP with no side reaction. We also noticed the evolution H_2 gas during the reaction. These bubbles would severely impede the optical measurements because their presence leads to a shift of the UV–vis spectra and a slight loss of the isosbestic points.

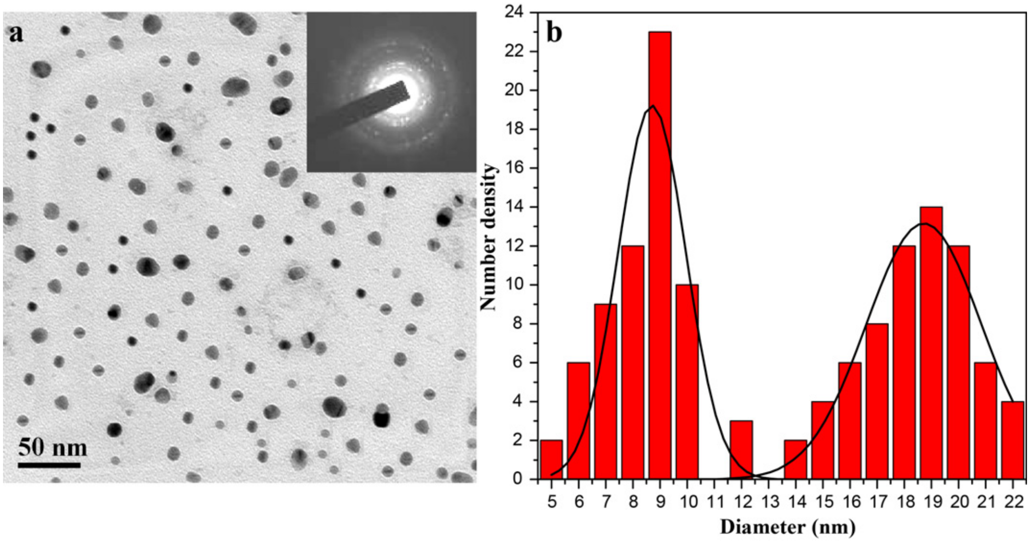

Fig. 2. (a) TEM micrograph of silver nanoparticles synthesized from 1 mM $AgNO_3$ (inset shows SAED pattern of the corresponding silver nanoparticles). (b) Particles size distribution histogram of silver nanoparticles determined from TEM images.

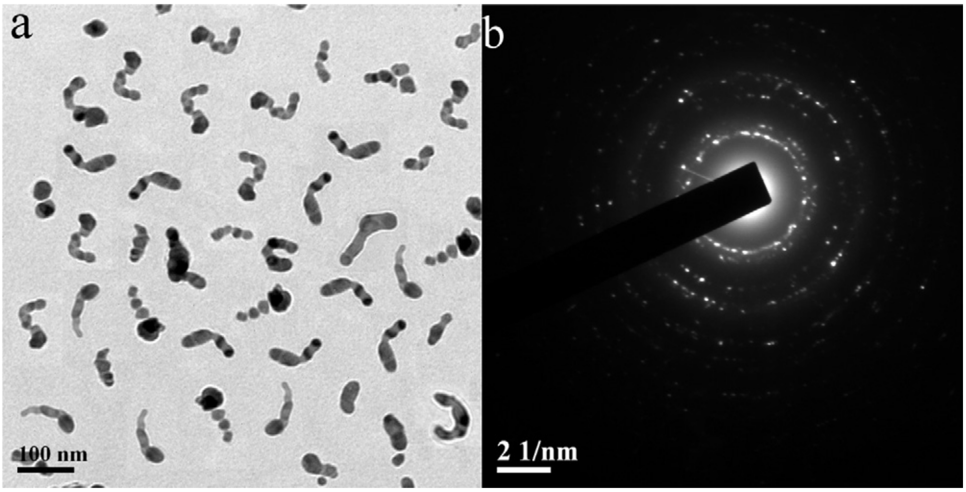

Fig. 3. (a) TEM micrograph of silver nanoparticles synthesized from 10 mM $AgNO_3$ (b) SAED pattern of the corresponding nanoparticles.

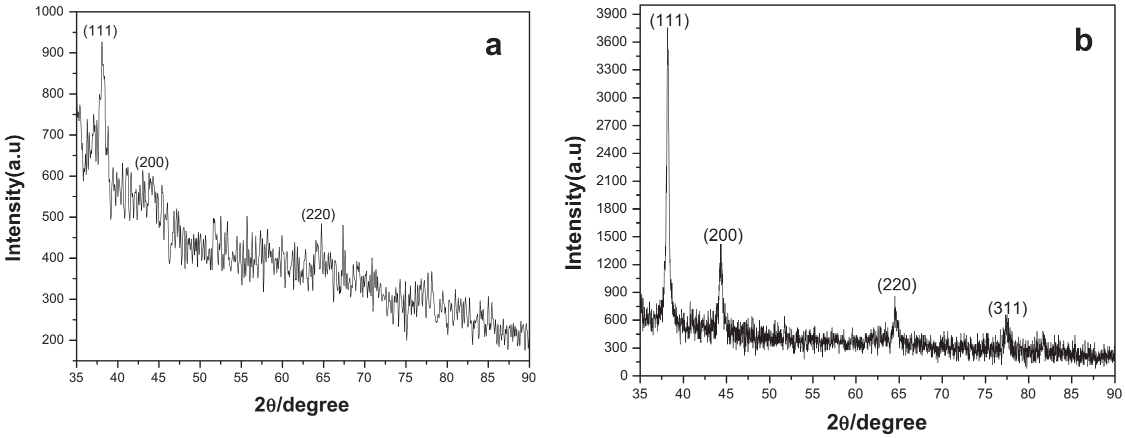

Fig. 4. XRD pattern of silver nanoparticles synthesized from (a) 1 mM $AgNO_3$ and (b) 10 mM $AgNO_3$.

In the absence of AgNPs, the solution containing p-NP and $NaBH_4$ shows absorption band with maxima at ~400 nm and this band correspond to the p-nitrophenolate ion under alkaline condition. No change of the above 400 nm band in the absence of AgNPs with time suggests the positive role AgNPs as catalyst. However, addition of a small amount (0.3 ml) AgNPs to the above reaction mixture with stirring causes fading and ultimate bleaching of yellow color of p-NP. A time-dependent UV–vis spectrum of these reaction mixtures shows the disappearance of the peak at 400 nm and is accompanied by a gradual development of a new peak at

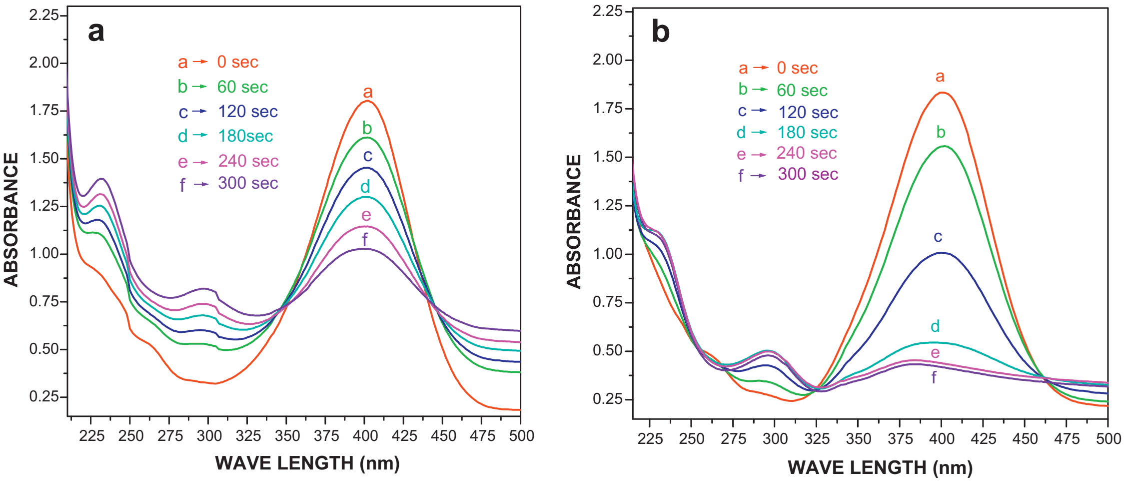

Fig. 5. UV–vis spectra of p-nitrophenol at different time interval during its reduction by $NaBH_4$ in presence of (a) spherical (b) worm like Ag nanoparticles as catalyst (initial reaction mixture: [p-NP] = 10 ml, 0.4 μM; [$NaBH_4$] = 0.10 ml, 0.3 M; [catalyst] = 0.3 ml).

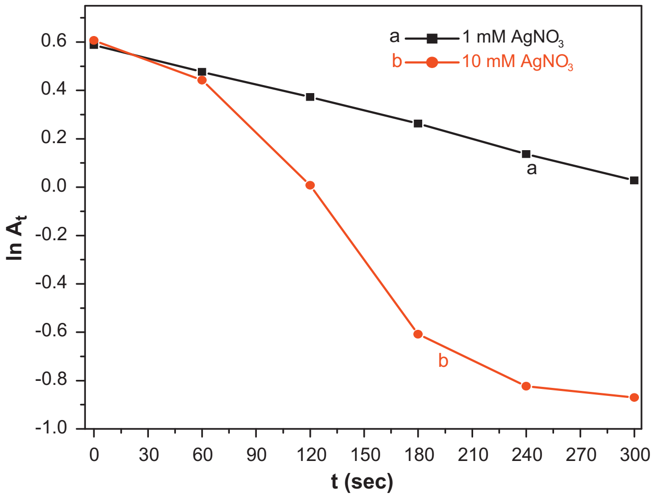

Fig. 6. Plots of '$\ln A_t$' vs. time 't' (s) for the reduction of p-nitrophenol to p-aminophenol by $NaBH_4$ in presence of (a) spherical and (b) worm like Ag nanoparticles as catalyst.

300 nm. This 300 nm band is due to the absorption of p-AP. It is also observed that catalytic activity of worm like Ag nanostructures is greater than the spherical shaped silver nanoparticles.

Present catalytic conversion of p-NP to p-AP follows the first order kinetics. In our reaction system, with the different shapes of silver nanocrystals, the reaction rate constant has been evaluated by plotting the '$\ln A_t$' versus time 't'; where A_t is absorbance at any time, 't'. The approximate linear relations of $\ln A_t$ versus 't' are observed for all the samples as shown in Fig. 6, support the first-order kinetics. The values of the calculated rate constants are $1.87 \times 10^{-3}\ s^{-1}$ for spherical nanoparticles and $3.37 \times 10^{-1}\ s^{-1}$ for worm like nanostructures. From the values of rate constants, it is clear that the rate is nearly 200 times faster for worm like nanostructures than spherical nanoparticles. We believe that the higher rate of reduction in worm like nanoparticles is due to the uneven surface of these anisotropic nanoparticles. The mechanism of the surface reaction was provided by Zhang, Li, and Chen (2009) by investigating the catalytic activity of Ag nanoclusters supported on TiO_2. They suggested that surface hydrogen is first transferred to the Ag nanoparticles by the decomposition of borohydride. This species then reacts with p-NP to yield the product p-AP. The reduction reaction is summarized in the following equation:

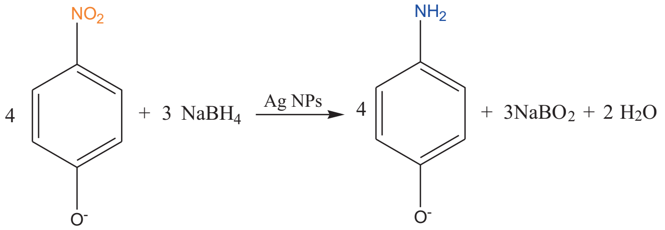

The kinetics of the reaction is modeled in terms of a Langmuir–Hinshelwood mechanism, where both reactants need to be adsorbed on the surface prior to reaction (Vannice, 2005; Xu, Kong, Yeh, & Chen, 2008). The mechanism is schematically displayed in Scheme 2. The rate-determining step is governed by the reaction of the adsorbed species. The adsorption/desorption equilibrium is assumed to be much faster and is modeled in terms of a Langmuir isotherm.

Again, the rate of reduction is independent of $NaBH_4$ concentration because this reagent used in excess compared to p-NP and the reaction rate follows first order kinetics (Ghosh, Mandal, Kundu, Nath, & Pal, 2004). So, the apparent rate constant K_{app} is proportional to the total surface 'S' of the nanoparticles (Lu, Mei, Ballauff, & Drechsler, 2006; Lu, Mei, Walker, Ballauff, & Drechsler, 2006; Mei et al., 2005).

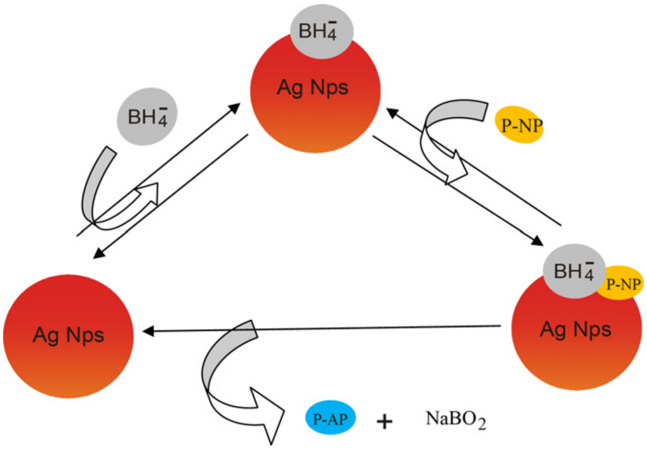

Scheme 2. Mechanistic model of Langmuir–Hinshelwood mechanism for the reduction of p-NP to p-AP by sodium borohydride in presence of Ag nanoparticles.

$$-\frac{dc_t}{dt} = K_{app}C_t = K_1SC_t \tag{1}$$

where C_t is the concentration p-NP at time t and K_1 is the rate constant normalized to S, the surface area of nanoparticles normalized to the unit volume of the system. Due to uneven surface of worm like AgNPs the total surface area for a given volume of nanosol is higher in worm like particle compared to spherical particle. This results the higher rate of catalytic activity of worm like AgNPs than that of spherical particles.

4. Conclusions

We have reported a simple one step method for the synthesis of worm like silver nanostructures and their catalytic activity. The silver nanostructures prepared in this present method can be stored at room temperature for nearly 6 months without any visible change. Reproducibility of the present synthesis suggests that this synthetic protocol can be used for the large scale production of silver nanostructure. We also investigated that the catalytic activity of AgNPs is greatly enhanced by the shape and size of nanocrystals. Due to the use of environmentally benign MC as template, it is also more helpful for the purpose of biomedical and pharmaceutical applications.

Acknowledgements

We gratefully acknowledge the financial support received from CSIR (Ref. No. 1427/NS-EMRII), New Delhi for carrying out this research work. The support rendered by Central research facility, IIT, Kharagpur, India for TEM measurements are gratefully acknowledged.

References

Andersson, M., Pederson, J. S., & Palmgrist, A. E. C. (2005). Silver nanoparticle formation in microemulsions acting both as template and reducing agent. *Langmuir*, *21*, 11387–11396.

Bawendi, M. G., Steigerwald, M. L., & Brus, L. E. (1990). The quantum mechanics of larger semiconductor clusters (quantum dots). *Annual Review of Physical Chemistry*, *41*, 477–496.

Bhui, D. K., Bar, H., Sarkar, P., Sahoo, G. P., De, S. P., & Misra, A. (2009). Synthesis and UV–vis spectroscopic study of silver nanoparticles in aqueous SDS solution. *Journal of Molecular Liquids*, *145*, 33–37.

Bhui, D. K., Pyne, S., Sarkar, P., Bar, H., Sahoo, G. P., & Misra, A. (2011). Temperature controlled synthesis of silver nanostructures of variable morphologies in aqueous methyl cellulose matrix. *Journal of Molecular Liquids*, *158*, 170–174.

Deheer, W. A. (1993). The physics of simple metal clusters: Experimental aspects and simple models. *Reviews of Modern Physics*, *65*, 611–676.

Esumi, K., Isono, R., & Yoshimura, T. (2004). Preparation of PAMAM- and PPI-metal (silver, platinum and palladium) nanocomposites and their catalytic activities for reduction of 4-nitrophenol. *Langmuir*, *20*, 237–243.

Ghosh, S. K., Mandal, M., Kundu, S., Nath, S., & Pal, T. (2004). Bimetallic Pt–Ni nanoparticles can catalyze reduction of aromatic nitro compounds by sodium borohydride in aqueous solution. *Applied Catalysis A*, *268*, 61–66.

Gobindaraj, A., Satishkumar, B. C., Nath, M., & Rao, C. N. R. (2000). Metal nanowires and intercalated metal layers in single-walled carbon nanotube bundles. *Chemistry of Materials*, *12*, 202–205.

Gou, L., Chipara, M., & Zaleski, J. M. (2007). Convenient, rapid synthesis of Ag nanowires. *Chemistry of Materials*, *19*, 1755–1760.

Gould, I. R., Lenhard, J. R., Muenter, A. A., Godleski, S. A., & Farid, S. (2000). Two-electron sensitization: A new concept for silver halide photography. *Journal of the American Chemical Society*, *122*, 11934–11943.

Hayakawa, K., Yoshimura, T., & Esumi, K. (2003). Preparation of gold–dendrimer nanocomposites by laser irradiation and their catalytic reduction of 4-nitrophenol. *Langmuir*, *19*, 5517–5521.

Jana, S., Ghosh, S. K., Nath, S., Pande, S., Praharaj, S., Panigrahi, S., et al. (2006). Synthesis of silver nanoshell-coated cationic polystyrene beads: A solid phase catalyst for the reduction of 4-nitrophenol. *Applied Catalysis A*, *313*, 41–48.

Jensen, T. R., Malinsky, M. D., Haynes, C. L., & Van Duyne, R. P. (2000). Nanosphere lithography: Tunable localized surface plasmon resonance spectra of silver nanoparticles. *The Journal of Physical Chemistry B*, *104*, 10549–10556.

Jin, R., Cao, Y., Mirkin, C. A., Kelly, K. L., Schatz, G. C., & Zheng, J. G. (2001). Photoinduced conversion of silver nanospheres to nanoprisms. *Science*, *294*, 1901–1903.

Kayanuma, Y. (1988). Quantum-size effects of interacting electrons and holes in semiconductor microcrystals with spherical shape. *Physical Review B*, *38*, 9797–9805.

Keki, S., Torok, J., Deak, G., Daroczi, L., & Zsuga, M. (2000). Silver nanoparticles by PAMAM-assisted photochemical reduction of Ag+. *Journal of Colloid and Interface Science*, *229*, 550–553.

Kreibig, U., & Vollmer, M. (1995). *Optical properties of metal clusters*. *Springer series in material science* Berlin: Springer.

Lin, J. C., & Wang, C. Y. (1996). Effects of surfactant treatment of silver powder on the rheology of its thick-film paste. *Materials Chemistry and Physics*, *45*, 136–144.

Liu, J. C., Qin, G. W., Raveendran, P., & Ikushima, Y. (2006). Facile green synthesis, characterization and catalytic function of β-D-glucose-stabilized Au nanocrystals. *Chemistry: A European Journal*, *12*, 2131–2138.

Liu, Y. C., & Lin, L. H. (2004). New pathway for the synthesis of ultrafine silver nanoparticles from bulk silver substrates in aqueous solutions by sonoelectrochemical methods. *Electrochemistry Communications*, *6*, 1163–1168.

Lu, Y., Mei, Y., Ballauff, M., & Drechsler, M. (2006). Thermosensitive core–shell particles as carrier systems for metallic nanoparticles. *Journal of Physical Chemistry B*, *110*, 3930–3937.

Lu, Y., Mei, Y., Walker, R., Ballauff, M., & Drechsler, M. (2006). 'Nano-tree'-type spherical polymer brush particles as templates for metallic nanoparticles. *Polymer*, *47*, 4985–4995.

Mallick, K., Witcomb, M. J., & Scurrell, M. S. (2005). Self-assembly of silver nanoparticles in a polymer solvent: Formation of a nanochain through nanoscale soldering. *Materials Chemistry and Physics*, *90*, 221–224.

Mann, S., & Ozin, G. A. (1996). Synthesis of inorganic materials with complex form. *Nature*, *382*.

Mei, Y., Sharma, G., Lu, Y., Drechsler, M., Ballauff, M., Irrgang, T., et al. (2005). High catalytic activity of platinum nanoparticles immobilized on spherical polyelectrolyte brushes. *Langmuir*, *21*, 12229–12234.

Narayanan, R., & El-Sayed, M. A. (2004). Changing catalytic activity during colloidal platinum nanocatalysis due to shape changes: Electron-transfer reaction. *The Journal of American Chemical Society*, *126*, 7194–7195.

Ozin, G. A. (1992). Nanochemistry: Synthesis in diminishing dimensions. *Advanced Materials*, *4*, 612–649.

Pradhan, N., Pal, A., & Pal, T. (2002). Silver nanoparticle catalyzed reduction of aromatic nitro compounds. *Colloids and Surfaces A: Physicochemical and Engineering Aspects*, *196*, 247–257.

Praharaj, S., Nath, S., Ghosh, S. K., Kundu, S., & Pal, T. (2004). Immobilization and recovery of Au nanoparticles from anion exchange resin: Resin-bound nanoparticle matrix as a catalyst for the reduction of 4-nitrophenol. *Langmuir*, *20*, 9889–9892.

Ramakrishna, G., & Ghosh, H. N. (2003). Optical and photochemical properties of sodium dodecylbenzenesulfonate (DBS)-capped TiO_2 nanoparticles dispersed in nonaqueous solvents. *Langmuir*, *19*, 505–508.

Rashid, M. H., Bhattacharjee, R. R., Kotal, A., & Mandal, T. K. (2006). Synthesis of spongy gold nanocrystals with pronounced catalytic activities. *Langmuir*, *22*, 7141–7143.

Ruan, D., Zhang, L., Zhang, Z., & Xia, X. (2004). Structure and properties of regenerated cellulose/tourmaline nanocrystal composite films. *Journal of Polymer Science B: Polymer Physics*, *42*, 367–373.

Sahoo, G. P., Bhui, D. K., Bar, H., Sarkar, P., Samanta, S., Pyne, S., et al. (2010). Synthesis and characterization of gold nanoparticles adsorbed in methyl cellulose micro fibrils. *Journal of Molecular Liquids*, *155*, 91–95.

Samanta, S., Pyne, S., Sarkar, P., Sahoo, G. P., Bar, H., Bhui, D. K., et al. (2010). Synthesis of silver nanostructures of varying morphologies through seed mediated growth approach. *Journal of Molecular Liquids*, *153*, 170–173.

Sandmann, G., Dietz, H., & Plieth, W. (2000). Preparation of silver nanoparticles on ITO surfaces by a double-pulse method. *Journal of Electroanalytical Chemistry*, *491*, 78–86.

Sarkar, P., Bhui, D. K., Bar, H., Sahoo, G. P., De, S. P., & Misra, A. (2009). Synthesis and photophysical study of silver nanoparticles stabilized by unsaturated dicarboxylates. *Journal of Luminescence*, *129*.

Sarkar, P., Bhui, D. K., Bar, H., Sahoo, G. P., Samanta, S., Pyne, S., et al. (2011). DDA-based simulation of UV–vis extinction spectra of Ag nanorods synthesized through seed-mediated growth process. *Plasmonics*, *6*, 43–51.

Schimd, G. (1992). Large clusters and colloids. Metals in the embryonic state. *Chemical Reviews*, *92*, 1709–1727.

Shipway, A. N., Lahav, M., & Willner, I. (2000). Nanostructured gold colloid electrodes. *Advanced Materials*, *12*(13), 993–998.

Sun, Y., Gates, B., Mayers, B., & Xia, Y. (2002). Crystalline silver nanowires by soft solution processing. *Nano Letters*, *2*, 165–168.

Sun, Y., Mayers, B., & Xia, Y. (2003). Transformation of silver nanospheres into nanobelts and triangular nanoplates through a thermal process. *Nano Letters*, *3*, 675–679.

Temgire, M. K., & Joshi, S. S. (2004). Optical and structural studies of silver nanoparticles. *Radiation Physics and Chemistry*, *71*.

Vannice, M. A. (2005). *Reactions*. Philadelphia, PA: Springer Science + Buisness Media.

Wang, Y., & Toshima, N. (1997). Preparation of Pd–Pt bimetallic colloids with controllable core/shell structures. *The Journal of Physical Chemistry B*, *101*, 5301–5306.

Wiley, B., Sun, Y., & Xia, Y. (2005). Polyol synthesis of silver nanostructures: Control of product morphology with Fe(II) or Fe(III) species. *Langmuir*, *21*, 8077–8080.

Xia, Y., Rogers, J. A., Paul, K. E., & Whitesides, G. M. (1999). Unconventional methods for fabricating and patterning nanostructures. *Chemical Reviews*, *99*(7), 1823–1848.

Xu, W., Kong, J. S., Yeh, Y-T. E., & Chen, P. (2008). Single-molecule nanocatalysis reveals heterogeneous reaction pathways and catalytic dynamics. *Nature Materials*, *7*, 992–996.

Yu, D., & Yam, V. W. (2004). Controlled synthesis of monodisperse silver nanocubes in water. *Journal of The American Chemical Society*, *126*, 13200–13201.

Zhang, D., Qi, L., Ma, J., & Cheng, H. (2001). Formation of silver nanowires in aqueous solutions of a double-hydrophilic block copolymer. *Chemistry of Materials*, *13*, 2753–2755.

Zhang, H., Li, X., & Chen, G. J. (2009). Ionic liquid-facilitated synthesis and catalytic activity of highly dispersed Ag nanoclusters supported on TiO_2. *Journal of Materials Chemistry*, *19*, 8223–8231.

Zong, R. L., Zhou, J., Li, Q., Du, B., Li, B., Fu, M., et al. (2004). Synthesis and optical properties of silver nanowire arrays embedded in anodic alumina membrane. *The Journal of Physical Chemistry B*, *108*, 16713–16716.